Stellar collisions in young star clusters

Gaburov, E.

Publication date
2008

Chapter 3

The present day mass function in the central region of the Arches cluster

Based on:
S. Portegies Zwart, E. Gaburov, H.-C. Chen and M. A. Gürkan
Monthly Notices of the Royal Astronomical Society, 378L, 29, 2007

ABSTRACT

We study the evolution of the mass function in young and dense star clusters by means of direct N-body simulations. Our main aim is to explain the recent observations of the relatively flat mass function observed near the centre of the Arches star cluster. In this region, the power law index of the mass function for stars more massive than about 5–6 $M_\odot$ is larger than the Salpeter value by about unity; whereas further out, and for the lower mass stars, the mass function resembles the Salpeter distribution. We show that the peculiarities in the Arches mass function can be explained satisfactorily without primordial mass segregation. We draw two conclusions from our simulations: 1) The Arches initial mass function is consistent with a Salpeter slope down to $\sim 1\ M_\odot$, 2) The cluster is about half way towards core collapse. The cores of other star clusters with characteristics similar to those of the Arches are expected to show similar flattening in the mass functions for the high mass ($\gtrsim 5\,M_\odot$) stars.

3.1 Introduction

The mass function of a star cluster changes because of both stellar evolution and stellar dynamics. Stellar evolution causes the turn-off mass to decrease as the most massive stars evolve away from the main sequence, ascend the giant branch to ultimately shed their envelopes to turn into compact objects. Stellar evolution therefore has a characteristic effect on the mass function by truncating it at the high mass end.

The dynamical evolution of a cluster has a more complicated effect on changes in the mass function. The dominant effect here is dynamical friction, which causes the most massive stars to sink to the cluster centre on a time scale that is inversely proportional to the stellar mass, i.e. the most massive stars tend to sink more quickly than relatively lighter stars. At the same time, stars less massive than the average mass tend to leave the inner regions. As a result of this *mass segregation*, the local stellar population becomes a function of the distance to the cluster centre.

Mass segregation, though mostly noticeable in the cluster's central regions, is a global phenomenon. A star cluster that is born with the same mass function across its radial coordinate will gradually grow a top-heavy mass function in its centre and a top-depleted mass function in its outskirts. Near the half mass radius, the mass function remains closest to the initial mass function (Vesperini & Heggie, 1997).

In this chapter, we concentrate on the evolution of the stellar mass function in the inner part of young and dense star clusters, using N-body simulations. Our interest in this topic was initiated by the recent accurate measurements published by Stolte et al. (2005); Kim et al. (2006) in which the mass function in the inner ~ 10" from the centre of the Arches star cluster was studied. These observations, especially the latter, revealed that the mass function of near the centre of Arches cluster is a broken power law, with the turning point $m_{\rm p} \sim 5{-}6 M_{\odot}$. We were able to reproduce this feature without invoking any special mechanism. Our simulations allow us to draw conclusions on the history of the dynamical evolution of the Arches cluster.

3.2 Dynamical evolution of the mass function

3.2.1 Parameters for the simulations

As a cluster evolves, stars more massive than the mean mass $\langle m \rangle$ tend to sink to the cluster centre whereas lighter stars move outwards. For the most massive stars, the time scale for dynamical friction is proportional to two-body relaxation time, $t_{\rm r}$:

$$t_{\rm df} \propto \frac{\langle m \rangle}{m_{\star}} t_{\rm r}, \tag{3.1}$$

were $m_\star$ is the mass of the massive star, which segregates inwards. The value of the relaxation time at the cluster's half-mass radius, r_h is given by (Spitzer, 1987, eq. 2.63)

$$t_\mathrm{r} = \frac{0.138N}{\ln\Lambda}\left(\frac{r_\mathrm{h}^3}{GM}\right)^{1/2}. \tag{3.2}$$

Here G is Newton's constant of gravity, M and N are the total mass and the number of stars in the cluster and $\ln\Lambda$ is the Coulomb logarithm, for which we adopt $\ln\Lambda = \ln(0.01N)$ (Giersz & Heggie, 1996). For the central relaxation time, we use

$$t_\mathrm{rc} = \frac{\sigma_\mathrm{3D}^3}{4.88\pi\, G^2 \ln\Lambda\, n\langle m_c\rangle^2}, \tag{3.3}$$

where σ_3D, n and $\langle m_c\rangle$ are the three-dimensional velocity dispersion, number density and average stellar mass at the cluster centre (Spitzer, 1987, eq. 3.37).

We follow the dynamical evolution of our models by means of direct N-body simulations, which we carry out with the `starlab` software environment (Portegies Zwart et al., 2001). The calculations are performed on the GRAPE-6 special purpose computer (Makino et al., 1997; Makino, 2001).

Our numerical experiments are performed with $N = 12288$ and 24576 stars. For each N, we perform simulations starting with a full range of density profiles for which we chose King (1966) models with the dimensionless parameter W_0 ranging from 3 to 12. The mass function in our simulations is described by a power-law, $dN/dm = m^x$, where we adopt the Salpeter value for the index ($x = -2.35$), with masses ranging from $1\,\mathrm{M}_\odot$ to $100\,\mathrm{M}_\odot$. In this way, the total mass of simulated clusters is $M \simeq 5\cdot 10^4$, which is consistent with the mass of the Arches cluster. To validate our results, we carried out additional simulations with $N = 49152$ as well as with a Salpeter mass function with $0.1\,\mathrm{M}_\odot$ as the lower limit. It will turn out that the presence of a tidal field has little effect on the results, but reducing the lower limit of the initial mass function to $0.1\,\mathrm{M}_\odot$ has a profound effect on the results, as we discuss below. For clarity we mainly focus on the models with 12288 and 24576 stars. With these parameters, the relaxation time at the virial radius for the 12k models is about 360 N-body time units, whereas for the 24k models this is 625 N-body time units (see Heggie & Mathieu (1986)[1]).

The close proximity of the Arches cluster to the Galactic centre (Cotera et al., 1992, 1996) would seemingly require the simulations to include tidal effects. And for understanding the dynamics in the cluster outskirts or the evaporation time scale the tidal field will prove crucial. For studying

[1] For the definition of an N-body unit see `http://en.wikipedia.org/wiki/Natural_units`.

the evolution of the central region on the short time scale reported here, however, the tidal field has negligible effect. We support this statement by carrying out additional simulations which include the tidal field, and those show no discernible effect. We therefore focus on the results of simulations without a tidal field. This has the attractive side effect that it allows us to scale our results with respect to N. We also ignore the effects of stellar evolution. This approximation is justified since on the short lifetime of the cluster (2 ± 1 Myr) even the most massive stars remain on the main sequence, though some effect of the stellar mass loss at the top end of the mass function can be expected. For example, a $60\,\mathrm{M}_\odot$ zero-age main sequence star with solar metalicity loses about $3\,\mathrm{M}_\odot$ in its first ~ 2.4 Myr (Lejeune & Schaerer, 2001), which has a negligible effect on the slope of the mass function.

3.2.2 Dynamical evolution towards core collapse

In our simulations we identify the moment of core collapse as soon as a persistent binary forms with a binding energy of at least 100 kT (where the energy scale kT is defined by the condition that the total stellar kinetic energy of the system, excluding internal binary motion, is $\frac{3}{2}N\mathrm{kT}$). For a cluster with a mass function that is consistent with the observed mass function in young star clusters, core collapse occurs at a more or less constant fraction of the initial central relaxation time $t_{\rm cc} \sim 0.2 \pm 0.1 t_{\rm rc}$ (Portegies Zwart & McMillan, 2002; Gürkan et al., 2004). In Fig. 3.1 we plot the moment of core collapse as a function of the initial concentration of the cluster. The slight dependence of $t_{\rm cc}/t_{\rm rc}$ on W_0, as well as the offset between our results with those of Gürkan et al. (2004) is presumably mainly caused by their broader range of stellar masses ($0.2 < m/\mathrm{M}_\odot < 120$) in the initial mass function, whereas here we adopt an initial mass function with $1 < m/\mathrm{M}_\odot < 100$. An additional effect is expected from the difference in the number of stars. The simulations of Gürkan et al. (2004) were carried out with 10^6 particles. The systematic difference between our results from simulations with 12k and 24k stars shows that this also affects the results systematically. At this moment, however, we cannot quantify this effect.

Dynamical friction causes the massive stars to segregate to the cluster centre making the mass function flatter at the higher end, in this region, until the formation of a hard binary. In Figure 3.2 we illustrate the evolution of the mass function between $r_{\rm core}$ and $2r_{\rm core}$. We show the mass function at birth (top curve, the Salpeter mass function), halfway to core collapse and at core collapse (bottom curve). We denote the point around which the slope of the mass function changes by $m_{\rm p}$, and the power-law indices in higher and lower ends by $x_{\rm m<m_p}$ and $x_{\rm m>m_p}$, respectively. The apparent decrease in the number of stars in the mass function presented in Figure 3.2 is the result of the cluster becoming more concentrated which causes the adopted annulus ($r_{\rm core} < r < 2r_{\rm core}$) to become narrower.

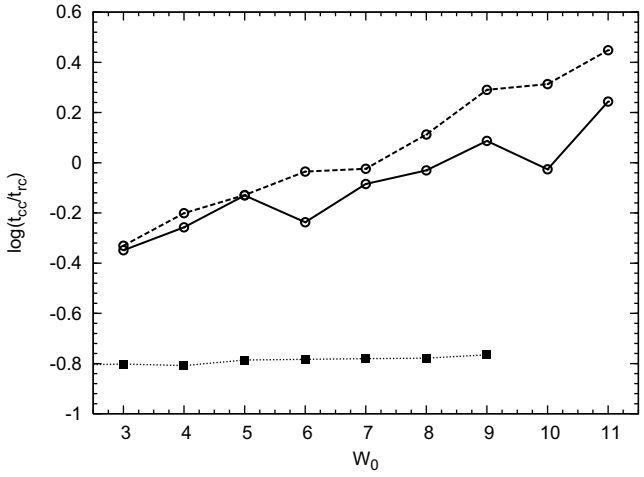

Figure 3.1: *The moment of core collapse ($t_{\rm cc}$) in units of the core-relaxation time ($t_{\rm rc}$) as a function of concentration parameter, W_0. The dashed curve gives the results of our simulations with 12k stars and the solid curve with 24k. Since we performed only one simulation per set of initial conditions no error bars are presented. The bottom (dotted) line denote the results of Gürkan et al. (2004).*

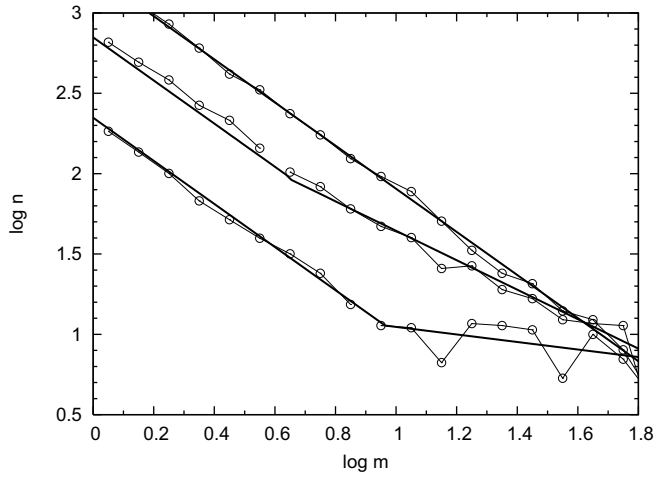

Figure 3.2: *The mass function of one of the simulations ($N = 24k$, $W_0 = 5$) for an annulus $1 < r/r_{\rm core} < 2$, around the cluster centre. From top to bottom, the curves are at times $t = 0$, $t \simeq 0.61 t_{\rm cc}$, and $t \simeq 1.05 t_{\rm cc}$. The solid lines are least squares fits to the mass function with a broken power-law.*

The effect of flattening of the mass function is less pronounced further away from the cluster centre. This is illustrated in Figure 3.3, where we present the evolution of $x_{\rm m>m_p}$ for the 24k simulations with $W_0 = 5$ and for $r = 0$ to $r_{\rm core}$ (top curve), for $r = r_{\rm core}$ to $2r_{\rm core}$ and for $r = 2r_{\rm core}$ to

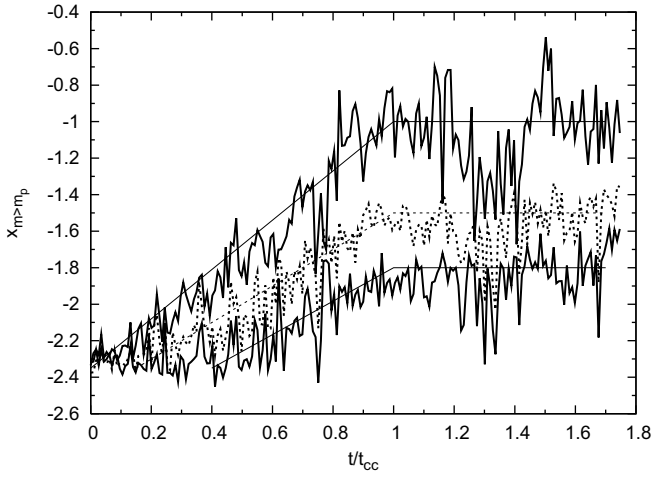

Figure 3.3: *The evolution of* $x_{\mathrm{m>m_p}}$ *for various radial bins in the 24k simulation with a* $W_0 = 5$ *King model. The time is given in units of core collapse time* t_{cc}*. The radial bins are* $0 < r/r_{\mathrm{core}} < 1$ *(upper solid curve),* $1 < r/r_{\mathrm{core}} < 2$ *(dotted curve), and* $2 < r/r_{\mathrm{core}} < 3$ *(lower solid curve). To guide the eye, we plotted straight lines through the simulation data.*

$3r_{\mathrm{core}}$ (bottom curve). The values of m_{p}, $x_{\mathrm{m<m_p}}$ and $x_{\mathrm{m>m_p}}$ are obtained by a three-point least squares fit to the mass function in a predetermined annulus of the simulated data. Note that we relaxed the fitting procedure in the sense that the mass function is not required to be continuous. The point of stalling of the evolution of the mass function can be identified by the moment of core collapse, regardless of the initial concentration or the number of stars in the simulation. Therefore, we normalize the time axis in Figure 3.3 to that instant.

3.2.3 Post-collapse mass function

After the formation of a hard binary, the mass function achieves a quasi steady state. The slope of the high-mass end of the mass function varies throughout the cluster. In Figure 3.4 we show how the mass function for stars with $m > m_p$ after the moment of core collapse is a function of the distance to the cluster centre, being flatter closer in and resembling the initial mass function further out. Overplotted are the observed values of the mass function exponent (see Tab. 3.1, see § 3.3). The results of our simulations without a tidal field are statistically identical to those with a tidal field. The simulations with a minimum mass to the initial mass function of $m_{\mathrm{min}} = 0.1\,\mathrm{M}_{\odot}$ is plotted as the thin dashed curve in Fig. 3.4. It may be noted that the results of simulations with $0.1\,\mathrm{M}_{\odot}$as the lower limit of the mass function are not consistent with the observed values of $x_{\mathrm{m>m_p}}$ and m_p.

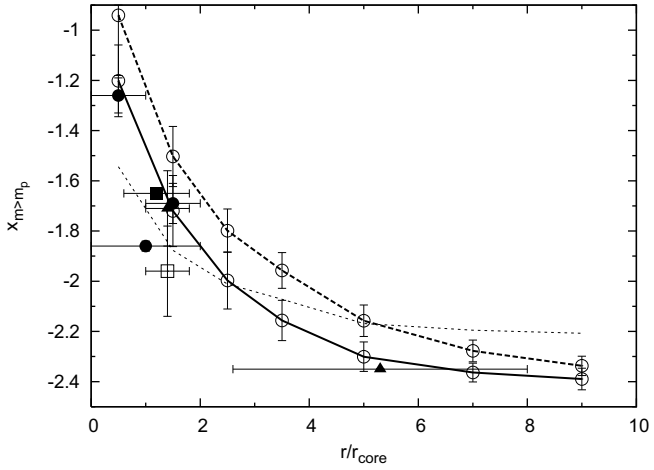

Figure 3.4: *The value of $x_{\mathrm{m}>\mathrm{m_p}}$ as a function of distance form the cluster centre after core collapse. The solid curve gives the average value of $x_{\mathrm{m}>\mathrm{m_p}}$ over the various simulations with 24k stars for $W_0 = 3$, 4, ... up to $W_0 = 12$, the thick dashed line gives the data for the simulations with $N = 12$k. The squares, bullets and triangles with error bars give the observed values taken from Figer et al. (1999), Stolte et al. (2005) and Kim et al. (2006), respectively (see Tab. 3.1). The thin dashed line gives the value of $x_{\mathrm{m}>\mathrm{m_p}}$ for simulations with 24k particles with $W_0 = 9$ and a lower limit to the initial mass function of 0.1 $\mathrm{M}_\odot$.*

In Figure 3.5, we show the value of m_p as a function of distance from the cluster centre for various simulations, past the moment of core collapse. It turns out that more concentrated initial models tend to result in a slightly smaller value of m_p whereas simulations with a smaller number of stars give rise to a higher value of m_p. The behaviour of $x_{\mathrm{m}>\mathrm{m_p}}$ is rather insensitive to the initial concentration of the cluster.

3.3 Mass function of the Arches cluster

At a projected distance of about 25 pc from Sgr A*, the Arches cluster ($\alpha = 17^h45^m50^s$, $\delta = -27°49'28''$ in J2000), discovered by Cotera et al. (1992, 1996), is peculiar. The total cluster mass is about $2 \cdot 10^4\,\mathrm{M}_\odot$. The core radius of the cluster (defined as the radial distance from the cluster centre where the luminosity profile drops by a factor two) is r_core= 5".0 (Stolte et al., 2005), and corresponds to about 0.2 pc if we assume that the distance to the Galactic centre is 8 kpc. The age of the cluster is 2 ± 1 Myr (Figer et al., 1999).

Recently, Kim et al. (2006) observed the Arches cluster using Keck/NIRC2 laser guide star adaptive optics. Their observations covered the inner parts of the cluster and some control fields at a distance of about 2.4 pc (60") from

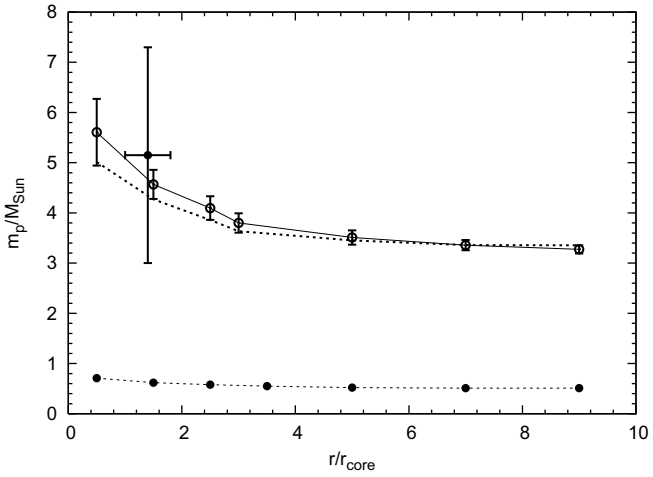

Figure 3.5: *The value of $m_{\rm p}$ after the point of core collapse, as a function of distance to the cluster centre for various of simulations. The open circles connected with the thin solid line give the results for the simulations with 24k stars and with $W_0 = 5$ averaged between the moment of core collapse and twice the core collapse time. The error bars indicate the variation of the value of $m_{\rm p}$ over this time period. More concentrated initial models tend to have a slightly lower value of $m_{\rm p}$, which we illustrate by plotting the $W_0 = 9$ simulation as the thick dotted line. The thin dashed line at the bottom gives the value of $m_{\rm p}$ for simulations with 24k particles with $W_0 = 9$ and a lower limit to the initial mass function of 0.1 $\rm M_\odot$.*

the cluster centre. They subsequently constructed the luminosity and mass functions down to about 1.3 $\rm M_\odot$, in an annulus of 5" (about 1.0 $r_{\rm core}$) to 9" (about 1.8 $r_{\rm core}$) from the cluster centre. In Table 3.1 we give the various measurements of the mass function and the distance from the cluster centre in terms of the observed core radius.

The data show that the slope in the mass function for stars more massive than $\sim 5\,\rm M_\odot$ flattens towards the cluster centre (see fig. 3.4). For lower mass stars, as well as for further out than $\sim 4\,r_{\rm core}$ it is closer to the Salpeter mass function. The observed mass function in the Arches is not a simple power-law (Stolte et al., 2005; Kim et al., 2006). We argue that in the inner parts of the cluster, $r \lesssim 4 r_{\rm core}$, the mass function is best described by two power laws with the break around $m_p = 5$–$6\,\rm M_\odot$. The mass function below this break (m_p) resembles the initial mass function ($x_{\rm m<m_p} \equiv x_{\rm IMF}$), and above m_p it becomes flatter ($x_{\rm m>m_p} > x_{\rm IMF}$). Further out than $r \simeq 4\,r_{\rm core}$ the break disappears and the mass function becomes gradually better represented with the initial mass function.

$r_{\rm min}$ ($r_{\rm core}$)	$r_{\rm max}$ ($r_{\rm core}$)	$m_{\rm min}$ ($\rm M_\odot$)	$m_{\rm max}$ ($\rm M_\odot$)	ref	x
0	1	12	60	1	-1.26 ± 0.07
1	2	6	16	1	-1.69 ± 0.08
1	2	16	60	1	-2.21 ± 0.09
0	2	6	60	1	-1.86 ± 0.02
1	1.8	6.3	50	2	-1.71 ± 0.15
1	1.8	1.3	50	2	-1.91 ± 0.08
0.6	1.8	6.3	125	3	~ -1.65
4	8	2.8	32	3	$\mathcal{O}(-2.35)$

Table 3.1: *Parameters for the observed mass function of the Arches cluster. The first two columns give the range over which the mass function is measured, in units of the cluster's core radius ($r_{\rm core} \simeq 0.20\,pc$). The third and fourth columns give the range in masses for which the exponent of the mass function (last column) is fitted. Column 5 gives the reference for the mass function exponents 1: Stolte et al. (2005), 2: Kim et al. (2006), 3: Figer et al. (1999), and the last column the measured value of x between $m_{\rm min}$ and $m_{\rm max}$.*

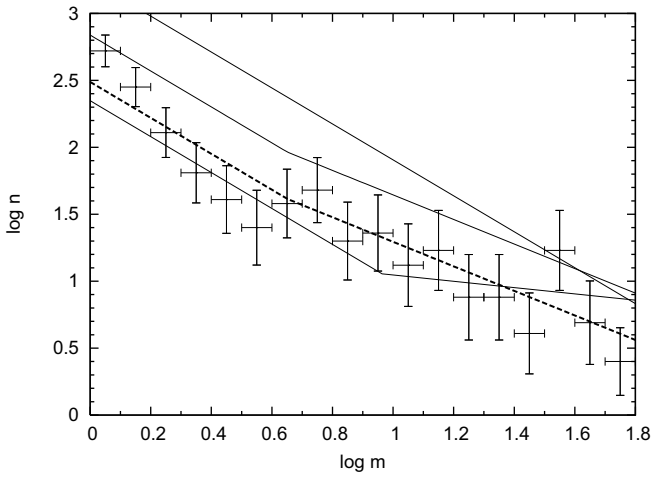

Figure 3.6: *The present day mass function of the Arches star cluster between $1\,r_{\rm core}$ and $1.8\,r_{\rm core}$. The error bars are taken directly from Fig. 5 of Kim et al. (2006). The three thin lines are from Fig. 3.2 at zero age (top line), at $t \simeq 0.61 t_{\rm cc}$ (middle line) and at $t \simeq 1.05 t_{\rm cc}$ (bottom line). The thick dashed line is identical to the thin $t \simeq 0.61 t_{\rm cc}$ but then renormalized with -0.35 dex. This line produces a satisfactory fit to the observed mass function.*

3.4 Discussion and conclusions

We performed detailed simulations of the evolution of young and dense star clusters using direct N-body simulations, in order to constrain the observed

mass function within about one parsec from the centre of the Arches cluster. The initial conditions of our simulations range over the full spectrum of King model density profiles.

The mass function in the central region of the Arches cluster is peculiar as it appears to be split in two power-laws, one for the stars less massive than 5–6 $M_\odot$ and a much shallower slope for the more massive stars. The two power-laws fit the observed data between 5" and 9" is marginally better ($\chi^2 \simeq 0.5$) than a single power-law ($\chi^2 \simeq 0.93$).

The simulations we perform to mimic the Arches cluster are able to reproduce this observed broken power-law mass function at the observed projected distance from the cluster centre ($r = 0$–$4\,r_{\rm core}$). The best comparison between observations and simulations is obtained if the cluster is about half way core collapse ($t = 0.4$–$0.6\,t_{\rm cc}$).

Our simulations, however, are performed without stellar evolution and without including the effects of an external tidal potential. As a result, they are scale-free, and no specific choices for the scalings to mass, size and therefore to time are obliged. However, the scale-free aspect of our simulations hinders the direct comparison to some extent as the size scale (in parsec) and time scale (in Myr) are important for an unbiased comparison with the observed Arches cluster.

In the comparison with the observations we adopt the same definition of the core radius by projecting the cluster and assigning luminosities of all stars in our simulations using zero-age main-sequence luminosities[2]. We ignore here the fact that very massive stars may become brighter in the 2 ± 1 Myr lifetime of the cluster, but this only affects the most massive stars, whereas the measurements are dominated by stars in the mid-range of masses.

The Arches cluster does not show any evidence for primordial mass segregation as our simulations (which were initialized without primordial mass segregation) are able to satisfactorily reproduce the observed mass function over the entire range of observed masses and distances from the cluster centre. Note also that the presence of primordial gas which failed to form stars does not seem to have affected the early cluster evolution, as the observed cluster structure at an age of 2 ± 1 Myr is satisfactory explained with the simulations, which do not include gas dynamics. The initial mass function of the Arches cluster is then consistent with a Salpeter slope between 1 $M_\odot$ and 100 $M_\odot$ without the need for a radial dependence. There seems to be no need for a large population of stars less massive than $\sim 1\,M_\odot$.

In Fig. 3.4 we show the evolution of $x_{\rm m>m_p}$ for the annuli and distances

[2]For comparison, we adopt the observers' definition of core radius: the point where the surface brightness drops to half its central value. This is similar to but different from definitions used in theoretical works of (Spitzer, 1987, eq. 1-34) and (Aarseth, 2003, eq. 15-4). In starlab we adopt the method as discussed by Heggie et al. (2006). The latter definition of the core radius systematically is about twice the observers' definition.

from the cluster centre reported from our compilation from the literature in Tab. 3.1. The best match between the simulations and the observations is acquired for simulations between $t = 0.4t_{\rm cc}$ and $0.6\,t_{\rm cc}$, i.e: we predict that the cluster is about half way towards core collapse. We therefore conclude that the Arches cluster has not yet experienced core collapse but is currently in a pre collapse stage.

In Tab. 3.1 we have quantified the slope to the low mass end of the mass function in 5" to 9" annulus of the Arches cluster as consistent with Salpeter, whereas the naive measurement in Fig. 5 of Kim et al. (2006) would results in $x_{\rm m<m_p} = -3.67 \pm 0.14$ (with $m_p = 5\,{\rm M}_\odot$), which is unusually steep. If this slope would represent the intrinsic Arches initial mass function and we adopt a minimum mass of $1\,{\rm M}_\odot$ the observed ~ 2600 stars more massive than $\sim 5\,{\rm M}_\odot$ in the Arches cluster would result in a total number of more than 2×10^5 stars, which is unrealistically high. From an observational point of view there are good arguments that the low mass end of the mass function is over-estimated, as it is plagued by selection effects. One of these effects is the artificial correction of missing stars in a crowded field and the selection of the three control fields to compensate for the background population. In the Keck observations these control fields are within about 2.4 pc from the cluster centre, which corresponds to $\sim 12\,r_{\rm core}$. For a King model with $W_0 \gtrsim 5.2$ the control fields would then be located near the cluster tidal radius. And since the cluster is about half way towards core collapse it is conceivable that the density profile is described with a King model with $W_0 \gtrsim 7$, in which case the control field are part of the cluster halo.

Due to mass segregation the cluster outskirts will be depleted of high mass stars and low mass stars will be overrepresented (the opposite effect as we discussed for the core population). Correcting the mass function in the cluster core with a population taken from near the cluster halo will therefore result in an enormous over correction towards the low mass stars, and consequentially result in a steepening of the 'corrected' mass function.

One of the control fields (field B of Kim et al, 2006) is taken near the location where one expects the tidal tail of the cluster in the potential of the Galaxy to pass though. The tidal tail is, since it consists of the halo population, also likely to be dominated by low mass stars.

Each of the effects discussed tend to steepen the lower-mass end of the mass function, though it is not trivial to quantize the effect without a much more detailed study. We however, argue that the initial mass function of the Arches cluster was probably consistent with Salpeter over the observed mass range. The observed break in the mass function around 5–6 ${\rm M}_\odot$ and the consequential flattening of the mass function for higher masses is then the result of the dynamical evolution of the cluster.

The initial model which is most comparable to the observed Arches cluster has a Salpeter initial mass function between $1\,{\rm M}_\odot$ and $100\,{\rm M}_\odot$ and with a reasonably concentrated initial density profile ($W_0 \gtrsim 4$ and $W_0 \lesssim 8$).

The break in the mass function in the inner parts of the cluster (for $r \lesssim 4r_{\rm core}$) appears at $m_{\rm p} \simeq 2\langle m \rangle$, which for our simulations is at about $5\,{\rm M}_\odot$. The break in the observed mass function in the Arches cluster appears around the same mass of $m_{\rm p} \simeq 5$–$6\,{\rm M}_\odot$. We performed additional simulations with $W_0 = 9$ using a Salpeter mass function down to $0.1\,{\rm M}_\odot$, and in this case the break in the core mass function also developed around $m_{\rm p} \simeq 2\langle m \rangle$, which for the adopted mass function is about $1.0\,{\rm M}_\odot$(Figure 3.5). Based on these findings we argue that the initial mass function in the Arches cluster has a lower limit of about $1.0\,{\rm M}_\odot$, as in our simulations that reproduce the observations best.

We predict that other clusters with similar parameters as the Arches cluster, like Westerlund 1 (Piatti et al., 1998), NGC 3603 (Moffat et al., 2004), R 136 (Meaburn et al., 1982) and Quintuplet (Cotera et al., 1992) will show similar characteristics as Arches. The mass functions in their cores will also be rather flat for stars more massive than 5–$6\,{\rm M}_\odot$. And the mass functions further away from the cluster centre will gradually be more like the initial mass function.

Acknowlegments

We are grateful to Peter Anders, Mark Gieles, Alessia Gualandris, Douglas Heggie and Henny Lamers for many discussions. This work was supported by NWO (grants #635.000.303 and #643.200.503), NOVA, the LKBF, the ISSI in Bern, Switzerland and the Taiwanese government (grants NSC095-2917-I-008-006 and NSC95-2112-M-008-006). MAG is supported by a Marie Curie Intra-European Fellowship under the sixth framework programme. The calculations for this work were done on the MoDeStA computer in Amsterdam, which is hosted by the SARA supercomputer centre.